

# Design and RTL-Level FPGA Realization of a MIMO-GFDM Digital Baseband Modem for Underwater Optical Wireless Communication

<sup>1</sup>V Tejavathi, <sup>2</sup>S Swarnalatha

<sup>1</sup>Research Scholar, <sup>2</sup>Professor

Department of Electronics and Communication Engineering, Sri Venkateswara University, Tirupati, India.

<sup>1</sup>[venatitejavathi@gmail.com](mailto:venatitejavathi@gmail.com), ORCID iD: [0009-0009-7098-3069](https://orcid.org/0009-0009-7098-3069),

<sup>2</sup>[swarnasvu09@gmail.com](mailto:swarnasvu09@gmail.com), ORCID iD: [0000-0001-6002-1389](https://orcid.org/0000-0001-6002-1389).

*\*Corresponding author: V Tejavathi*

**Abstract:** Underwater Wireless Communication (UWC) has emerged as an important enabling technology for applications including ocean observation, offshore monitoring, underwater sensor networks, assisted navigation, and Internet of Underwater Things (IoUTs). Among the available communication techniques, Underwater Optical Wireless Communication (UOWC) offers high data rates, low transmission latency, and improved bandwidth utilization for short- to medium-range communication scenarios. However, underwater optical channels remain affected by attenuation, scattering, and signal degradation, requiring bandwidth efficient transmission techniques. This paper presents the design and RTL-level FPGA realization of a Multiple-Input Multiple-Output Generalized Frequency Division Multiplexing (MIMO-GFDM) digital baseband modem for underwater optical wireless communication. The proposed architecture combines GFDM-based multicarrier transmission with MIMO processing to support flexible time–frequency allocation and reduced interference effects in underwater communication environments. The complete modem architecture is developed and evaluated using MATLAB/Simulink under simulated underwater channel conditions. To demonstrate implementation feasibility, the designed communication blocks are translated into synthesizable VHDL through an HDL-based workflow and analysed through RTL-level realization for FPGA-oriented implementation. Simulation outputs including transmitted and received signal behaviour, error characteristics, spectral response, and implementation resource observations are presented for performance assessment. The obtained results indicate that the proposed architecture provides an effective framework for investigating spectrally efficient underwater optical communication systems and demonstrates the feasibility of RTL-level realization for future hardware deployment.

**Keywords:** Underwater Optical Wireless Communication, MIMO, Generalized Frequency Division Multiplexing, Digital Baseband Modem, FPGA, RTL Design, MATLAB/Simulink, HDL.

## 1 INTRODUCTION

Underwater wireless communication has become an important technology for various marine and subsea applications, such as oceanographic monitoring, underwater sensor networks, autonomous underwater vehicles (AUVs), offshore infrastructure monitoring, and defence systems. Therefore, the increasing demand for reliable and high-speed underwater connectivity creates a need for transmission techniques that address the limitations of conventional underwater communication methods. Traditionally, underwater communication has relied on acoustic and radio-frequency (RF) techniques. Underwater acoustic communication (UAC) is widely used for long-distance transmission, but it suffers from primary constraints, such as limited bandwidth, low data rates, high latency and the effect of multipath fading [1]. In contrast, underwater RF communication experiences severe attenuation in seawater due to its high conductivity, limiting its transmission distance to only a few meters.

These limitations have motivated research into underwater optical wireless communication, which provides high-speed communication over short- to medium-distance. UOWC systems provide high bandwidth, low latency, high energy efficiency, and improved physical-layer security compared to acoustic and RF communication techniques. These characteristics of UOWC are used for high-data-rate applications, real-time video transmission, high-resolution sensing, and transfer of large volumes of stored data from devices in underwater environments. Still, underwater optical channels are severely affected by factors like absorption, scattering, and inter-symbol interference (ISI) [2]. Fig. 1 illustrates a typical UOWC scenario representing underwater entities communicating through optical links.

Overcoming these channel impairments requires advanced, bandwidth efficient modulation techniques to maintain reliable performance under highly dispersive, time-varying channel conditions. Several multicarrier modulation techniques have been explored, particularly Orthogonal Frequency Division Multiplexing (OFDM), which have been widely used in UOWC systems due to their ability to mitigate frequency-selective fading and provide equalisation [3].

Still, OFDM-based optical systems face different practical challenges, such as a high peak-to-average power ratio (PAPR), requirements of stringent orthogonality, high out-of-band emissions, and greater sensitivity to synchronisation errors. Due to these limitations, OFDM may become less suitable for bandwidth-constrained, power-sensitive underwater optical links.

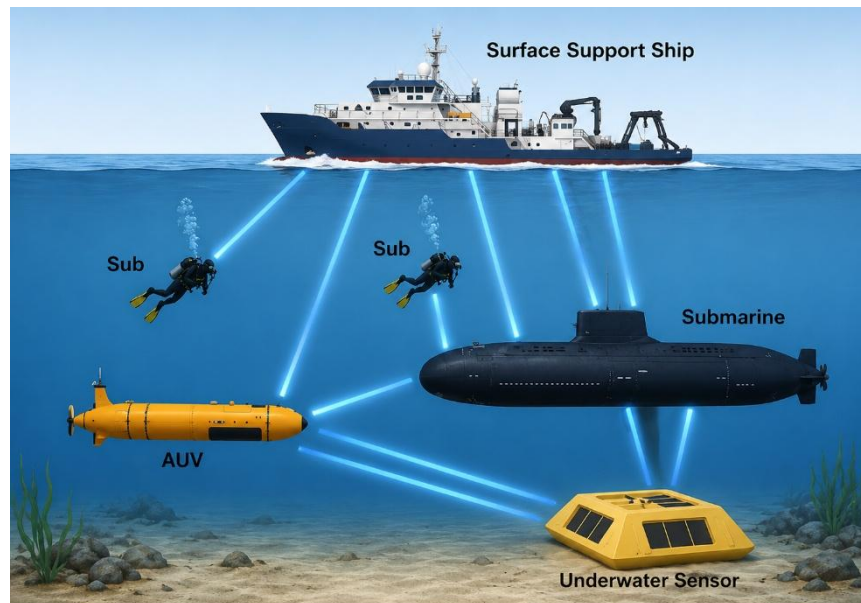


Fig. 1. Typical Application Scenarios of UWOC

Although UOWC research has progressed significantly, most current systems still depend on OFDM techniques. Also, MIMO techniques are widely used in regular wireless systems in terrestrial environments; their integration with underwater optical communication remains an active research area in underwater optical communication, especially when combined with multicarrier modulation techniques and tested for real-time hardware implementation [4]. This motivates the investigation of Generalised Frequency Division Multiplexing (GFDM) as a promising alternative modulation approach.

GFDM is a block-based multicarrier modulation technique that uses circular pulse shaping and improved spectral efficiency. Compared to OFDM, GFDM offers low out-of-band emission, high spectral efficiency, and greater reduction of ISI and inter-carrier interference (ICI). These parameters make GFDM particularly useful for limited- bandwidth applications and for dispersive underwater optical channels. In addition, using MIMO techniques provides spatial diversity and spatial multiplexing, which improve link reliability, spectral efficiency, and bit-error rate (BER) performance. Compared to existing single-input single-output (SISO) systems and MIMO-OFDM systems, a MIMO-GFDM system offers greater robustness to underwater optical channel impairments and better spectrum utilisation.

This paper presents a MIMO-GFDM-based underwater optical wireless communication modem intended to support bandwidth efficient transmission and investigate communication performance under simulated underwater conditions. This work focuses on system-level design and RTL-oriented implementation analysis. The complete MIMO-GFDM-based UOWC system is first designed and implemented in MATLAB Simulink to verify its functionality and evaluate its performance under realistic underwater optical channel conditions. After simulation-level verification, synthesizable VHDL is generated from the Simulink model and analysed through RTL-level realization for FPGA-oriented implementation. Register Transfer Level (RTL) schematics are analysed to understand the architecture and internal data flow of the proposed optical modem. By combining algorithm design, system simulation, and FPGA-implementation, this approach demonstrates the feasibility of integrating algorithm-level design with HDL-oriented realization for underwater wireless communication applications. The main contributions of this work are summarized as follows:

- Design of a MIMO-GFDM digital baseband modem for underwater optical wireless communication using MATLAB/Simulink.
- Investigation of transmitted signal behaviour, spectral response, and error characteristics under simulated underwater communication conditions.
- HDL-oriented realization of the proposed modem architecture through synthesizable VHDL generation and RTL-level FPGA implementation analysis.
- Comparative evaluation of the proposed MIMO-GFDM configuration with SISO-GFDM and MIMO-OFDM configurations under identical simulation conditions.

The rest of the paper is organised as follows. Section 2 presents literature survey, section 3 presents working principle of underwater optical wireless communication. Section 4 outlines the methodology adopted for underwater optical wireless communication. Section 5 describes the implementation of the MIMO-GFDM-based underwater optical modem. Section 6 presents the simulation and synthesis results obtained from MATLAB Simulink and Xilinx environments. Section 7 concludes the paper and identifies potential directions for future research.

## 2 LITERATURE SURVEY

UWC is increasingly used in applications such as oceanographic observation, autonomous underwater vehicle (AUV) operations, sensor networks, and subsea infrastructure monitoring. Traditional underwater communication mainly relies on acoustic and radio-frequency methods, both of which exhibit practical limitations under underwater conditions. Acoustic systems provide long-range communication, but they suffer from low bandwidth, high propagation delay, and susceptibility to environmental noise [2]. RF signals attenuate rapidly in conductive seawater because EM waves do not propagate well in water. Due to this, the transmission distance of RF communication is very short, a few meters. Optical wireless communication (OWC) has emerged as a promising option for supporting higher data-rate underwater links [5], [6]. Developments in UOWC have increased bandwidth, data rates, and energy efficiency [7].

Still, UOWC performance is distorted by absorption, scattering, turbulence, and ISI in the underwater channel [8]. To mitigate these channel effects, multicarrier modulation techniques, particularly OFDM, have become more popular in UOWC research [9], [10]. OFDM is effective under frequency-selective fading conditions and reduces the need for equalisation, but it has a high peak-to-average power ratio, sensitivity to synchronisation, and spectral leakage, which create implementation challenges in underwater environments [11], [12]. Recent research has studied alternative multicarrier techniques, such as GFDM and filter bank multicarrier (FBMC), for UOWC [13], [14]. GFDM employs circular pulse shaping and has been reported to reduce out-of-band emissions while improving flexibility in time–frequency allocation [15]. Incorporating MIMO techniques with advanced modulation approaches has been investigated to enhance spectral utilization and communication robustness in underwater optical systems [16], [17].

Recent developments have placed greater focus on hardware implementation and the practicality of these next-generation schemes. Several studies have explored FPGA-oriented implementation approaches for communication modem realization [18]. J. Li et al. reported FPGA-oriented realization for underwater optical communication applications, demonstrating that hardware implementation is feasible and effective in underwater environments [19]. R. Hema et al. investigated MIMO-based OFDM techniques for underwater optical wireless communication systems and analysed communication performance under underwater channel conditions [20]. M. Murad et al. discussed practical approaches for MIMO-GFDM-based underwater modems, mainly focusing on system-level considerations for real-world implementation [21]. Z. Li et al. discusses implementation-oriented considerations for GFDM-based communication systems [22].

Recent contributions [23]–[26] describe bit-error rate, power efficiency, and system bandwidth for optical modems using GFDM for long-distance underwater and next-generation wireless systems, indicating the potential of these technologies for future high-performance UOWC. Motivated by these studies, this work investigates the design and RTL-level realization of a MIMO-GFDM-based digital baseband modem under simulated underwater optical communication conditions. Unlike studies that primarily focus on algorithm-level evaluation, this work additionally considers HDL-oriented realization and implementation feasibility through generated RTL structures.

## 3 WORKING PRINCIPLE OF UNDERWATER OPTICAL WIRELESS COMMUNICATIONS

A UOWC system consists of three main components: the transmitter, the underwater channel, and the receiver, as shown in Fig. 2. The transmitter (TX) comprises a modulator, an optical driver, a light source, and a projection lens. The receiver (RX) consists of an optical bandpass filter, a photodetector, low-noise electronics, and a demodulator. The transmitter consists of a modulator and pulse-shaper unit, an optical driver, a light source, and a projection lens.

Conventional modulation techniques require adaptation for practical optical communication systems; intensity modulation techniques commonly adopted in optical communication systems, including ON-OFF Keying (OOK) and Non-Return-to-Zero ON-OFF Keying, are widely used because of their simple and practical implementation. Multicarrier modulation techniques, such as OFDM with QPSK and QAM signalling, have also been analysed to enable higher data rates. The electrical signal is converted into an optical signal using optical transmit elements such as LEDs or laser diodes, and the emitted light is shaped by a suitable projection lens. Underwater optical systems are typically designed using either a diffuse line-of-sight or a point-to-point line-of-sight configuration, as shown below in Fig. 3.

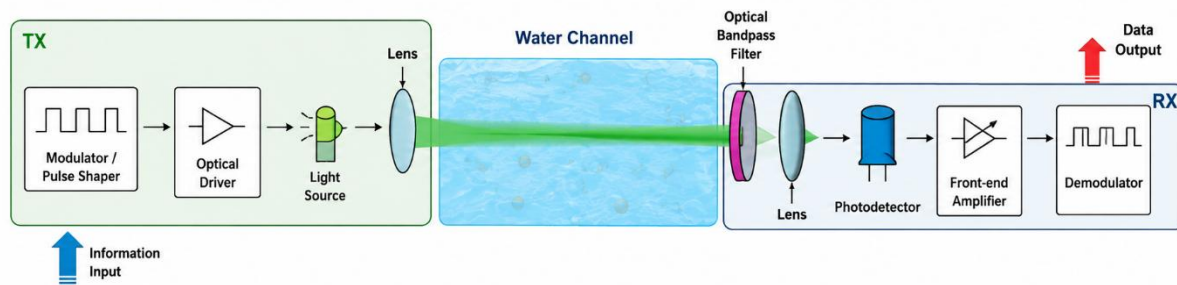


Fig. 2. Schematic of a Typical UOWC Link

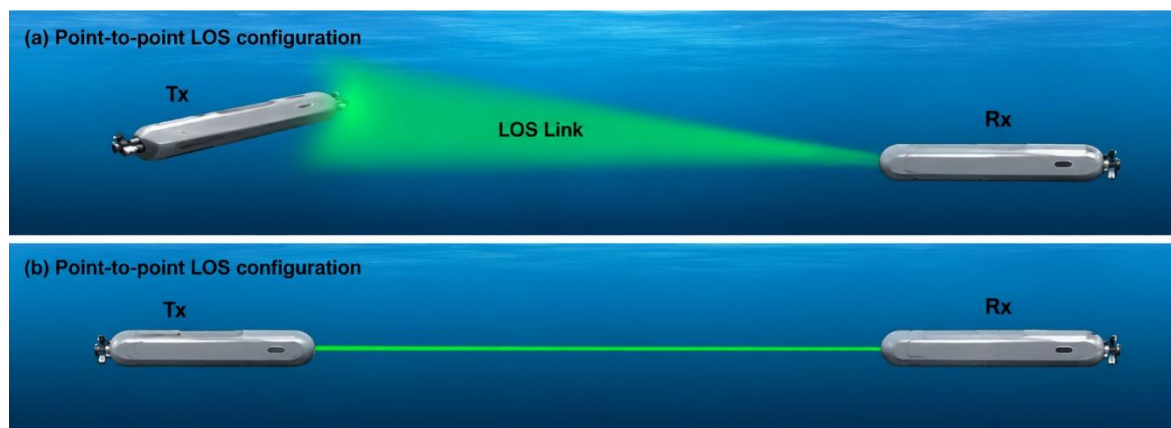


Fig. 3. Example Link Configurations of Different Underwater Optical Wireless Communication

Diffuse LOS configurations use wide-beam LEDs for short-range broadcast communication, but they suffer severe attenuation and limited data rates. On the other hand, Point-to-point LOS configurations generally employ narrow-beam optical transmission to support higher data rates and directional communication, but they require perfect alignment between transmitter and receiver. Projection lenses are used to control beam divergence and improve optical coupling. In the receiver section, a narrow optical band-pass filter is present to suppress background light and noise from the incoming signal. The filtered optical signal is converted into an electrical signal using a photodetector. Generally, photodiodes are either PIN or avalanche photodiodes.

The performance of these photodiodes in long-distance UOWC systems is limited by noise and attenuation. Recent studies have examined single-photon avalanche diodes (SPADs), which operate in Geiger mode and provide high sensitivity, improved detection accuracy, and low noise. The recovered electrical signal is then demodulated to reconstruct the transmitted data. In this work, the communication chain is represented at the digital baseband level and evaluated under simulated underwater channel conditions to study implementation feasibility.

## 4 METHODOLOGY

### 4.1. Generalised Frequency Division Multiplexing

GFDM is a flexible block-based multicarrier modulation technique that has been investigated for next-generation wireless communication systems. GFDM supports flexible time–frequency allocation and has been studied for improving spectral utilization. In GFDM, data symbols are transmitted in blocks composed of subcarriers and subsymbols. GFDM employs circular pulse shaping with block-based transmission and is intended to reduce out-of-band emissions while supporting efficient spectrum usage, as shown in Fig. 4. In comparison, OFDM typically employs orthogonal subcarriers with rectangular pulse shaping.

In GFDM, each subcarrier is shaped using a circular pulse-shaping approach, and in this work a root-raised cosine (RRC) filter configuration is considered, through circular convolution. This pulse-shaping approach may reduce spectral leakage and improve spectral containment, thereby reducing the out-of-band emissions and improving energy efficiency while maintaining bandwidth. In the GFDM transmitter, the input bit stream is converted into complex symbols by using modulation techniques such as QPSK or M-QAM. These symbols are arranged into a two-dimensional time–frequency grid. Each sub-symbol is pulse-shaped using a prototype filter that is circularly shifted in time and modulated in frequency for each subcarrier. The filtered sub-symbols are then summed to generate a single GFDM block.

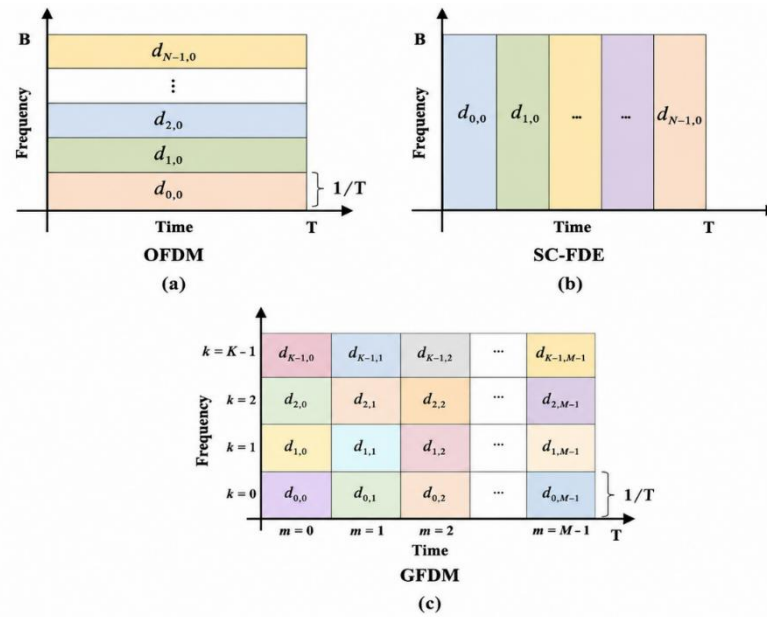


Fig. 4. GFDM Time-Frequency Grid Structure

The discrete-time GFDM transmit signal is expressed as

$$x[n] = \sum_{k=0}^{K-1} \sum_{m=0}^{M-1} d_{k,m} g_{k,m}[n] \quad (1)$$

where  $d_{k,m}$  represents transmitted data symbols,  $g_{k,m}[n]$  represents the pulse-shaping function,  $K$  denotes the number of subcarriers, and  $M$  denotes the number of subsymbols. A cyclic prefix (CP) is added to each block to mitigate channel-induced ISI and to enable efficient frequency-domain equalisation. Following CP removal, equalization and signal recovery are performed using conventional receiver processing approaches to recover the transmitted symbols. Owing to its flexible pulse shaping and block structure, GFDM has been reported to provide improved spectral containment under suitable configurations, increased robustness to synchronisation errors, and enhanced spectral efficiency compared to conventional OFDM. These characteristics motivate the investigation of GFDM for bandwidth-constrained and dispersive underwater communication scenarios. At the receiver, demodulation and signal reconstruction are performed through the implemented processing chain to recover the transmitted symbols. The circular pulse shaping and flexible time–frequency allocation inherent to GFDM contribute to reduced out-of-band emissions and increased robustness against inter-symbol interference.

#### 4.2. Simulation Parameters

To improve reproducibility and maintain consistency across simulation and implementation stages, the principal parameters used for modelling and evaluating the proposed MIMO-GFDM digital baseband modem are summarized in Table 1. The selected parameters correspond to the MATLAB/Simulink configuration and the HDL-oriented realization flow adopted in this work. These settings were used to observe transmitted and received signal behaviour, evaluate error characteristics, and analyse implementation feasibility under simulated underwater communication conditions.

Table 1. Simulation Parameters used for MIMO-GFDM Modem Evaluation

S. No.	Parameter	Configuration
1	Communication Mode	Optical
2	Modulation Technique	16-QAM
3	Pulse Shaping Filter	Root Raised Cosine (RRC)
4	Simulation Platform	MATLAB/Simulink
5	HDL Realization	VHDL
6	Channel Model	Simulated Underwater Channel
7	Eb/No Range	5–65 dB
8	Maximum Number of Bits	4352

The above configuration provides a common simulation environment for evaluating the behaviour of the proposed communication architecture and supporting RTL-level implementation analysis.

### 5 PROPOSED MIMO-GFDM BASED OPTICAL MODEM DESIGN USING MATLAB SIMULINK

This work proposes and implements a MIMO-GFDM-based optical modem in MATLAB/Simulink for UOWC systems. The transmitter and receiver architecture are developed to investigate communication behaviour and implementation feasibility under simulated underwater optical communication conditions. Fig. 5 shows the MATLAB/Simulink model of the proposed MIMO-GFDM digital baseband modem architecture.

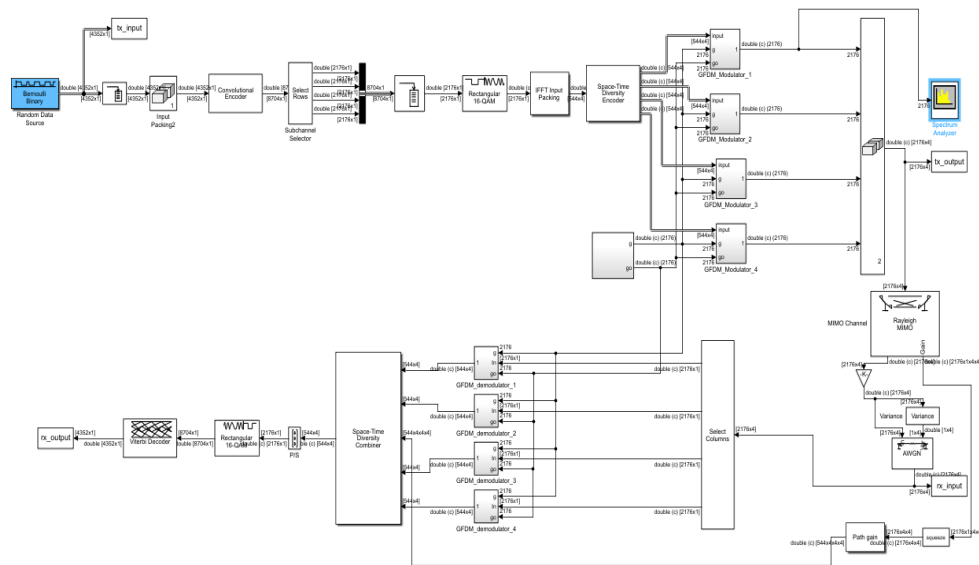


Fig. 5. Proposed MIMO-GFDM-Based Optical Modem Design Using MATLAB/Simulink

#### 5.1. GFDM Transmitter Section

In this transmitter, a random binary data stream is generated using a Bernoulli binary block. The generated binary stream is applied to a convolution encoder to introduce redundancy for improved signal recovery at the receiver. This stage supports error correction during signal reconstruction under simulated channel impairments. The data streams from the convolution encoder are given to the 16-QAM modulator. The encoded data are mapped into complex symbols using 16-QAM modulation. IFFT is performed on each complex symbol. The output of the IFFT block is given to the space-time diversity encoder, which uses an Alamouti coding scheme. The Alamouti space-time diversity encoder provides transmit diversity by distributing symbols across multiple transmission paths.

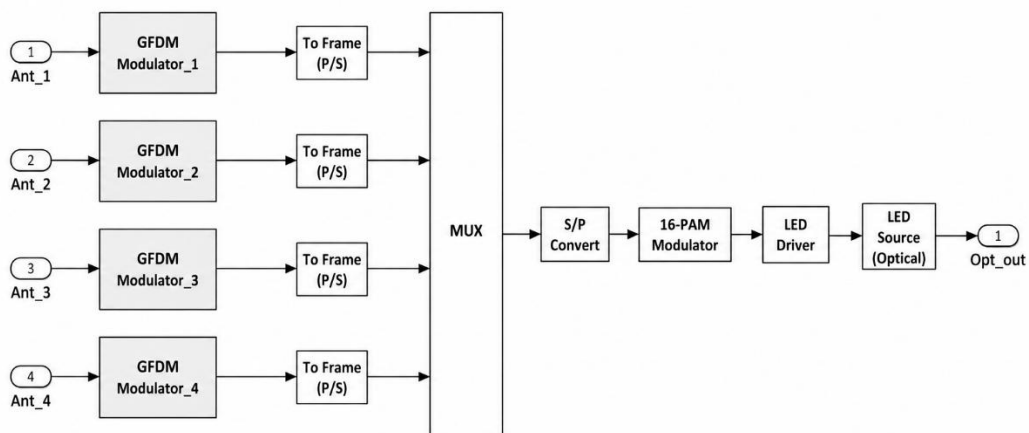


Fig. 6. Schematic Diagram of the Proposed MIMO-GFDM Transmitter Section.

This stage supports diversity-oriented transmission while maintaining the communication bandwidth. The output of the space-time diversity encoder is applied to different GFDM modulators.

Each GFDM subsystem comprises a root-raised cosine filter, which shapes the transmitted pulses so that symbols do not interfere with each other while satisfying the Nyquist criterion for zero ISI, thereby supporting controlled pulse shaping and signal formation. After performing the pulse shaping, these pulses are applied to the GFDM block. The GFDM configuration is selected through simulation and summarized in Table 1. The resulting GFDM signal is then processed through a MIMO space-time diversity encoder, enabling spatial processing across multiple optical transmission branches. Fig. 6 illustrates the schematic structure of a MIMO-GFDM transmitter section.

### 5.2. Modelling Optical Channel

The transmitted GFDM signal is processed through simulated channel blocks representing underwater communication effects. Mathematically, this channel is expressed as

$$r(t) = h(t) * g(t) \tag{2}$$

where  $h(t)$  represents the Rayleigh-distributed fading coefficient and  $g(t)$  is transmitted GFDM signal. The adopted channel abstraction is intended to emulate signal variation and attenuation behaviour under simulated underwater communication conditions. Rayleigh fading is incorporated within the simulation framework to represent channel variability during signal propagation. The combination of variance and gain blocks represents the large-scale attenuation experienced by the optical signal during underwater propagation. In underwater wireless optical communication, signal power decays exponentially with distance due to absorption and scattering, and this behaviour can be approximated using attenuation modelling based on Beer–Lambert behaviour. Mathematically, it is expressed as

$$P_r = P_t e^{-cd} \tag{3}$$

where ‘c’ represents the attenuation coefficient and ‘d’ represents the propagation distance. These blocks represent signal attenuation and power variation during propagation. The gain and variance blocks are used to represent attenuation and signal-strength variation within the adopted simulation environment. The AWGN block models the receiver and ambient noise present in underwater optical wireless communication systems. In the adopted simulation framework, noise effects are represented using equivalent simulation-based noise components associated with photodetector and receiver behaviour. These noise sources collectively exhibit random behaviour that can be well approximated as Additive White Gaussian Noise (AWGN). Accordingly, the received signal can be expressed as

$$y(t) = [h(t) * g(t)]e^{-cd} + n(t) \tag{4}$$

where  $n(t) = N(0, \sigma^2)$  represents additive white Gaussian noise introduced within the adopted simulation environment.

### 5.3. GFDM Receiver Section

At the receiver section, the received GFDM signal is first applied to the GFDM demodulator, where it first undergoes an FFT, and then it reshapes the pulses by using circular shifting. After that, it is applied to a space-time diversity combiner.

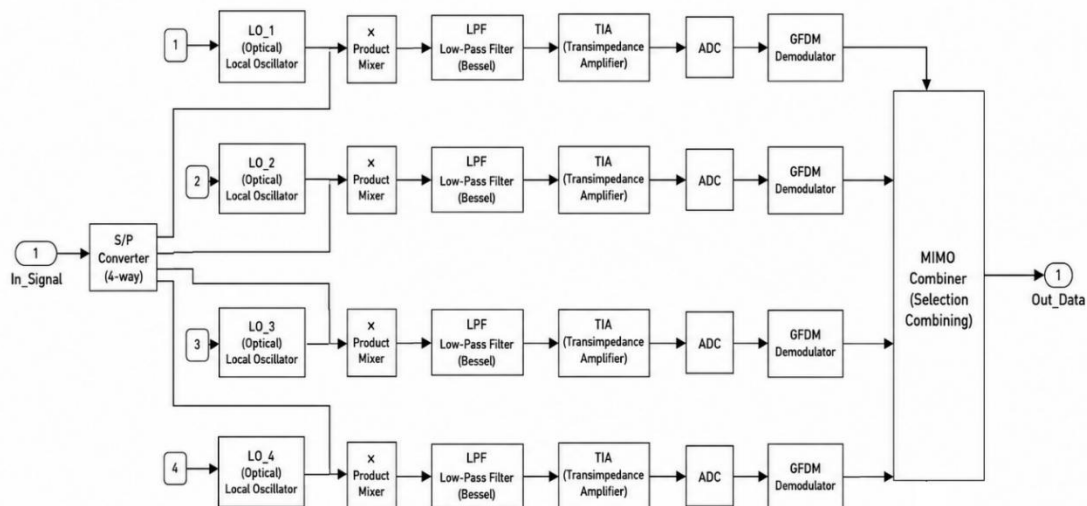


Fig. 7. Schematic Diagram of the Proposed MIMO-GFDM Receiver Section

The diversity combiner performs signal reconstruction across the received transmission branches to achieve diversity gain. Without a space-time diversity combiner, the benefits of space-time encoding (such as Alamouti coding) cannot be realised at the receiver. The output of the space-time diversity combiner is applied to the 16-QAM demodulator, which converts the complex symbols into data streams. The recovered data streams are then applied to the Viterbi decoder. This Viterbi algorithm is used to decode convolutionally encoded data by determining the most likely transmitted bit sequence from the received noisy signal. It improves error correction capability and supports reconstruction of transmitted information in communication systems. Fig. 7 shows the schematic structure of a MIMO-GFDM receiver section. The complete communication chain was implemented and evaluated within MATLAB/Simulink and subsequently translated through an HDL-oriented workflow to support RTL-level realization and implementation analysis.

## 6 SIMULATION AND SYNTHESIS RESULTS

### 6.1. MATLAB Simulation Results

The proposed MIMO-GFDM digital baseband modem was designed and evaluated using MATLAB/Simulink under simulated underwater optical communication conditions. In this digital baseband modem, the communication channel was represented using simulation blocks intended to emulate attenuation, channel variation, and noise effects for underwater optical communication analysis. The attenuation-related effects were represented through the adopted simulation configuration, and additional signal variation behaviour was incorporated within the simulation framework. The combined behaviour of these blocks approximates attenuation characteristics represented through Beer-Lambert modelling. Noise behaviour was represented through simulation-based noise components based on the photodetector responsivity and receiver bandwidth. Therefore, transmitted and received signal behaviour, error characteristics, spectral response, and power-related observations were obtained through MATLAB/Simulink under simulated underwater optical channel conditions. Fig. 8 and 9 display the input and output signals of the GFDM system.

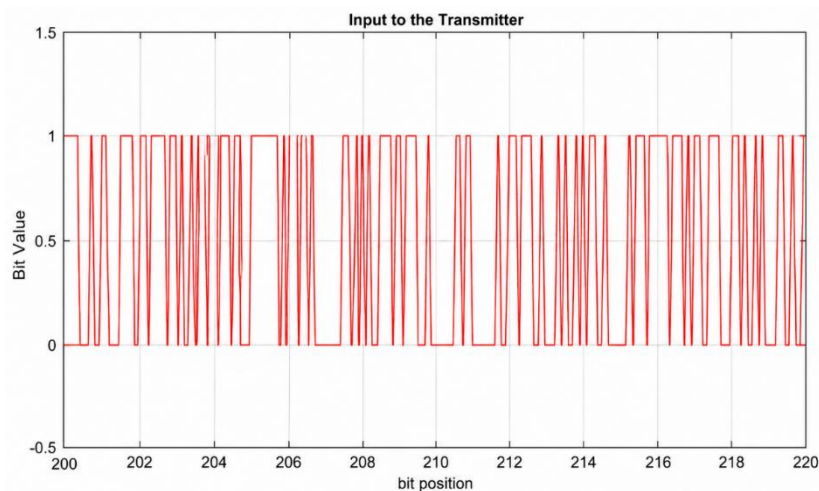


Fig. 8. Input to the Transmitter

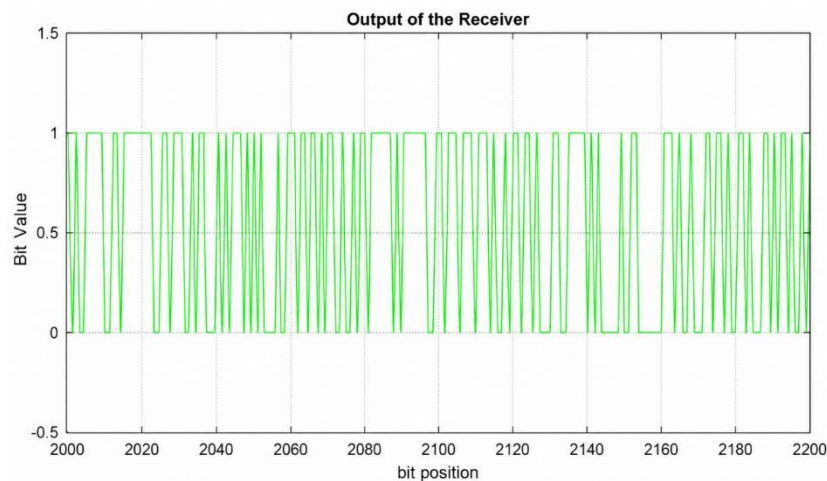


Fig. 9. Output of the Receiver

The transmitted and received signal plots indicate that the implemented GFDM communication chain successfully reconstructs the transmitted bit sequence under the adopted simulation conditions. Minor variations observed in the received waveform are associated with the simulated channel and noise effects incorporated within the communication framework. Fig. 10 and 11 present the error characteristic plot and power spectral response. Fig. 12 shows the power analysis obtained from the simulation environment.

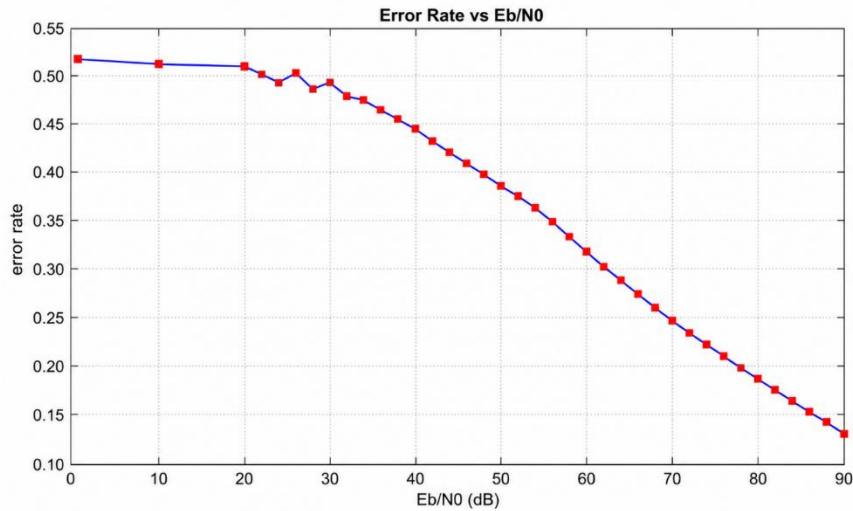


Fig. 10. Error Metric versus Eb/N0 Plot for Optical Signal

The error characteristic curve illustrates the variation of the simulation-derived error metric with increasing Eb/No values. A gradual reduction in the reported error values can be observed as the signal conditions improve within the adopted simulation environment.

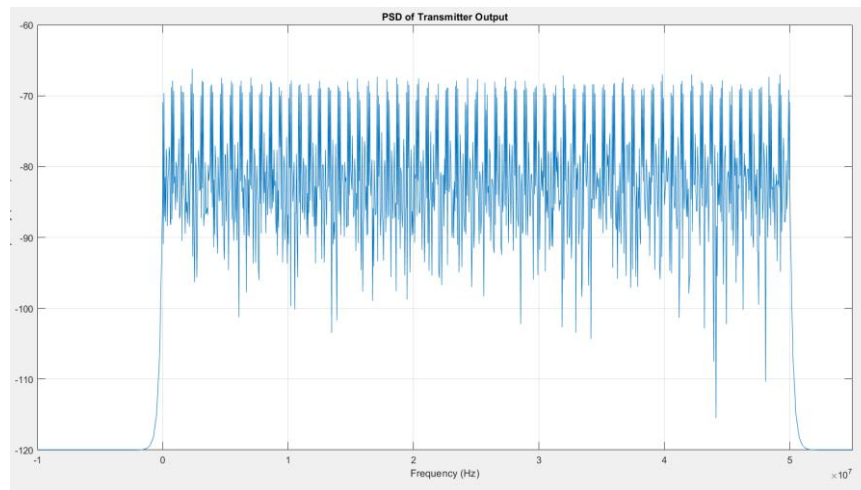


Fig. 11. Power Spectral Density of the MIMO-GFDM Digital Baseband Modem

The PSD response demonstrates the spectral distribution of the transmitted GFDM waveform and indicates controlled spectral behaviour within the simulated digital baseband communication framework.

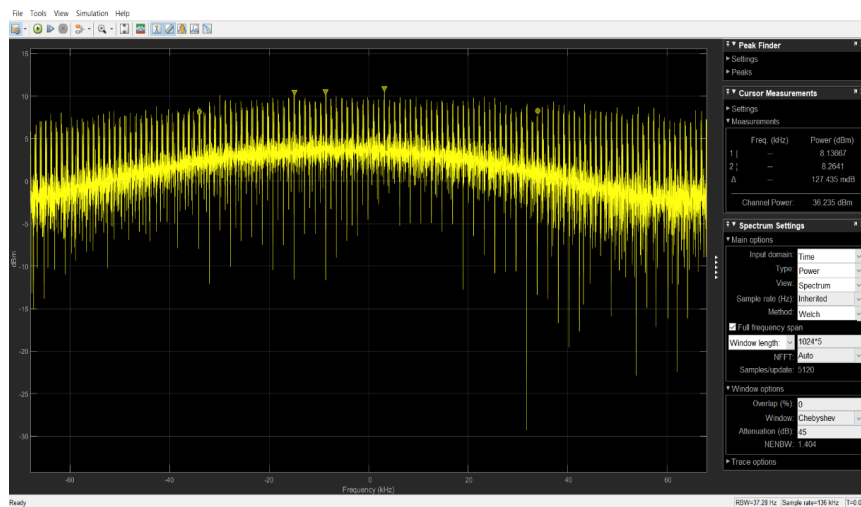


Fig. 12. Power Analyser Output of the MIMO-GFDM Digital Baseband Modem

Quantitative observations related to transmitted power, received power, signal current, noise characteristics, and signal-to-noise ratio obtained from the simulation environment are summarized in Table 2.

Table 2. Simulated Performance Observations of the Proposed MIMO-GFDM Modem

S. No.	Parameter	MIMO GFDM
1.	Electrical Power (W)	4.20 W
2.	Optical Tx Power (30%)	1.26 W
3.	Received Optical Power (10 m)	62.7 mW
4.	Signal Current	25.1 mA
5.	Shot Noise	0.63 $\mu$ A
6.	Thermal Noise	0.91 $\mu$ A
7.	Total Noise Current	1.11 $\mu$ A
8.	Theoretical SNR	87.1 dB
9.	Practical SNR (with margins)	60–65 dB
10.	Error Metric (Simulation Output)	0.4105

Error values correspond to simulation output comparison under identical operating conditions and are presented for relative performance evaluation. Table 3 presents a comparison between MIMO-GFDM, SISO-GFDM, and MIMO-OFDM.

Table 3. Comparative Simulation-level Observations of MIMO-GFDM, SISO-GFDM and MIMO-OFDM

S. No.	Parameter	MIMO-GFDM	SISO-GFDM	MIMO-OFDM
1	Electrical Power (W)	4.20 W	7.13 W	8.38 W
2	Optical Tx Power (30%)	1.26 W	2.14 W	2.51 W
3	Received Optical Power (10 m)	62.7 mW	106 mW	125 mW
4	Signal Current	25.1 mA	42.4 mA	50 mA
5	Shot Noise	0.63 $\mu$ A	0.82 $\mu$ A	0.89 $\mu$ A
6	Thermal Noise	0.91 $\mu$ A	0.91 $\mu$ A	0.91 $\mu$ A
7	Total Noise Current	1.11 $\mu$ A	1.22 $\mu$ A	1.27 $\mu$ A
8	Theoretical SNR	87.1 dB	90.8 dB	91.9 dB
9	Practical SNR (with margins)	60–65 dB	65–70 dB	65–72 dB
10	Error Metric (Simulation Output)	0.4105	0.49	0.51

These comparative observations are intended to provide implementation-level insight into the relative behaviour of the investigated communication configurations under identical simulation assumptions. The electrical power consumption of MIMO-GFDM is 4.20 W, which is significantly lower than 7.13 W for SISO-GFDM presented in [22] and 8.38 W for MIMO-OFDM presented in [21], indicating lower reported transmission requirements within the adopted configuration.

The comparison indicates that the proposed MIMO-GFDM configuration exhibits lower reported error values and reduced simulated power observations relative to the compared configurations. Under the adopted simulation conditions, the proposed architecture reports an error metric of 0.4105 compared with 0.49 for SISO-GFDM and 0.51 for MIMO-OFDM. These observations support comparative evaluation of the proposed communication framework.

### 6.2. Xilinx Synthesis Results

Following MATLAB simulation, each block was translated into VHDL code and synthesised using Xilinx ISE 14.7. The synthesis results for both the MIMO-GFDM transmitter (TX) and receiver (RX) sections are presented in Fig. 13 and Fig. 14, illustrating RTL and technology-level realization generated through the HDL workflow. Each block was translated into VHDL code and synthesized into RTL and technology schematics for implementation-oriented analysis.

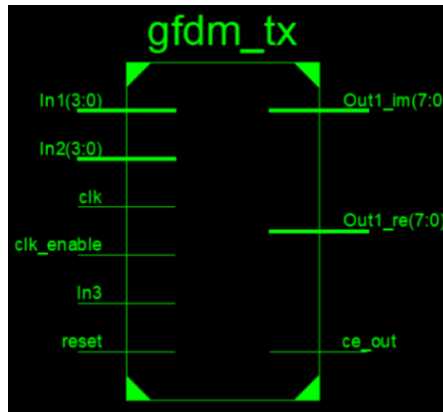


Fig. 13. RTL schematic for MIMO-GFDM TX Section

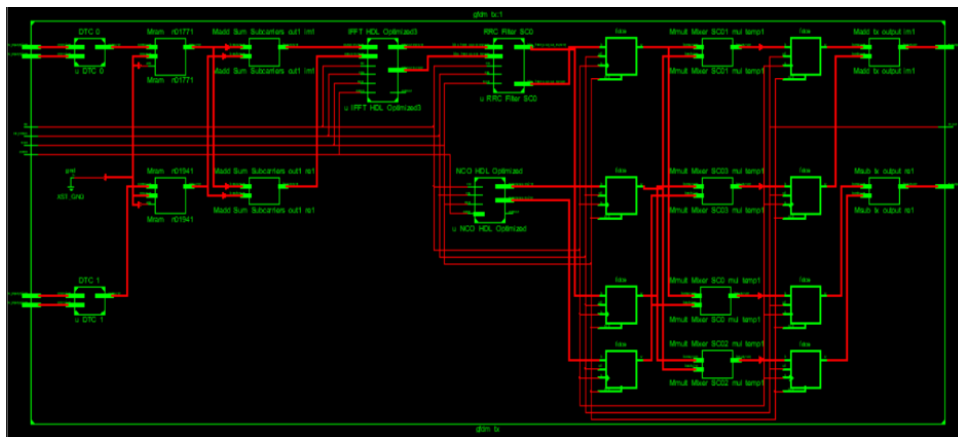


Fig. 14. Technology schematic for MIMO-GFDM TX Section

Similarly, Fig. 15 and Fig. 16 show the RTL schematic and Technology Schematic of a MIMO-GFDM Receiver Section.

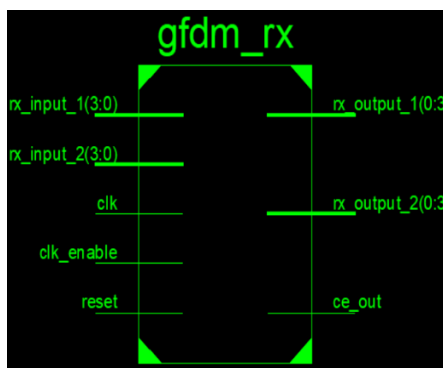


Fig. 15. RTL schematic for MIMO-GFDM RX Section

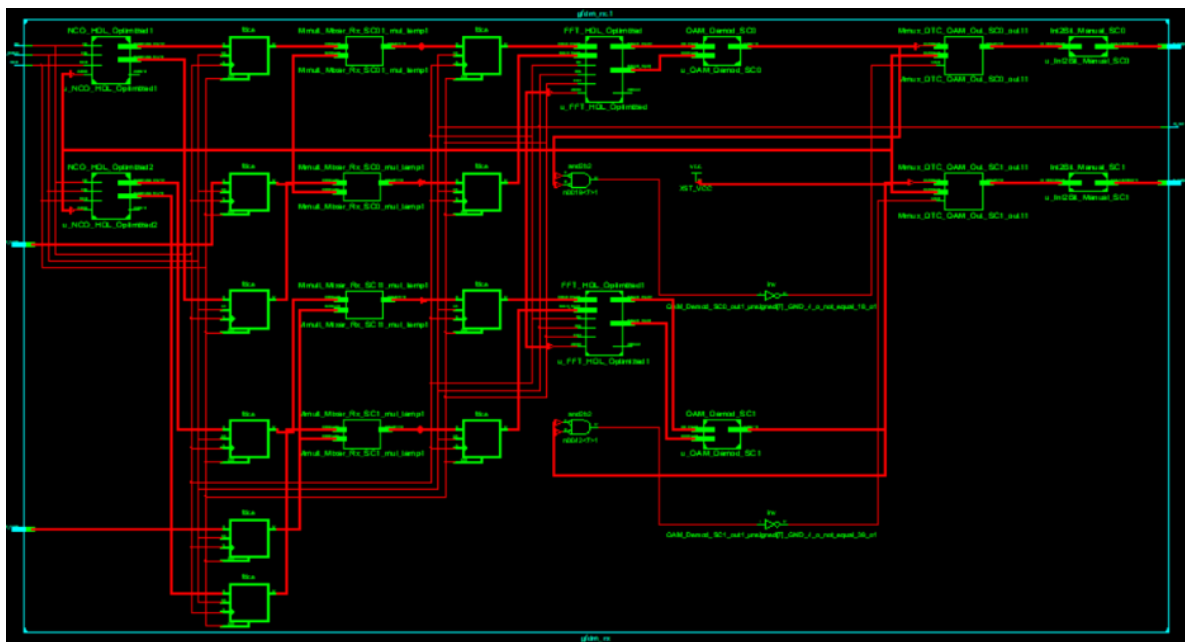


Fig. 16. Technology schematic for MIMO-GFDM RX section

The generated RTL and technology schematics provide structural visualization of the synthesized communication architecture and support implementation-oriented analysis of the proposed modem design. Below is the FPGA Resource Utilisation Summary Table 4, generated directly from Xilinx 14.7 synthesis reports for both the transmitter and the receiver. Target device is Spartan-6 (xc6slx9-2-tqg144).

Table 4. FPGA Resource Utilisation Summary

S. No.	Resource	Used	Available	Utilisation (%)
1	Slice LUTs	1597	5720	27%
2	Slice Registers (Flip-Flops)	1956	11440	17%
3	DSP48A1 Slices	16	16	100%
4	LUT RAM (Memory as LUT)	150	1440	10%
5	Bonded IOBs	21	102	20%
6	BUFG (Clock Buffers)	1	16	6%
7	Maximum Operating Frequency	58.051 MHz	—	—

The synthesis summary indicates that the generated HDL architecture can be accommodated within the selected FPGA resource limits. Full utilization of DSP resources suggests that arithmetic processing contributes significantly to implementation complexity, while available logic resources indicate the possibility of further functional expansion.

## 7 CONCLUSIONS

The design and RTL-level realization of a MIMO-GFDM digital baseband underwater optical wireless communication modem are presented, utilising MATLAB/Simulink for system development and Xilinx ISE 14.7 for HDL synthesis and implementation analysis. Simulation results show that the proposed MIMO-GFDM system exhibits lower reported error values and comparative communication performance relative to SISO-GFDM and MIMO-OFDM configurations under the adopted simulation conditions. The error characteristics, PSD, and power analysis indicate stable spectral behaviour and signal transmission performance under simulated underwater channel conditions. In addition, VHDL generated from the Simulink model and synthesized in Xilinx ISE 14.7 demonstrates the feasibility of realizing the digital baseband modem through an FPGA-oriented implementation workflow. The proposed architecture supports spectrally efficient communication and implementation feasibility while maintaining reduced simulated power observations under the adopted configuration. The presented framework may be considered for short- to medium-range underwater optical communication studies. The present work is limited to simulation-based underwater channel modelling and RTL-level implementation analysis without physical underwater experimentation. Future work will focus on integrating physical optical front-end components and experimental realization in real underwater environments.

**FUNDING INFORMATION**

This research received no specific grant from any funding agency in the public, commercial, or not-for-profit sectors.

**ETHICS STATEMENT**

This study did not involve human or animal subjects and, therefore, did not require ethical approval.

**STATEMENT OF CONFLICT OF INTERESTS**

The authors declare no conflicts of interest related to this study.

**LICENSING**

This work is licensed under a [Creative Commons Attribution 4.0 International License](https://creativecommons.org/licenses/by/4.0/).

**REFERENCES**

- [1] F. Akyildiz, D. Pompili, and T. Melodia, "Underwater acoustic sensor networks: research challenges," *Ad Hoc Networks*, vol. 3, no. 3, pp. 257–279, Feb. 2005, doi: 10.1016/j.adhoc.2005.01.004.
- [2] K. Y. Islam, I. Ahmad, D. Habibi, and A. Waqar, "A survey on energy efficiency in underwater wireless communications," *Journal of Network and Computer Applications*, vol. 198, p. 103295, Dec. 2021, doi: 10.1016/j.jnca.2021.103295.
- [3] M. Stojanovic, "Underwater Acoustic Communications: Design Considerations on the Physical Layer," *2008 Fifth Annual Conference on Wireless on Demand Network Systems and Services*, Garmisch-Partenkirchen, Germany, 2008, pp. 1-10, doi: 10.1109/WONS.2008.4459349.
- [4] X. Che, I. Wells, G. Dickers, P. Kear and X. Gong, "Re-evaluation of RF electromagnetic communication in underwater sensor networks," in *IEEE Communications Magazine*, vol. 48, no. 12, pp. 143-151, December 2010, doi: 10.1109/MCOM.2010.5673085.
- [5] H. Kaushal and G. Kaddoum, "Underwater Optical Wireless Communication," in *IEEE Access*, vol. 4, pp. 1518-1547, 2016, doi: 10.1109/ACCESS.2016.2552538.
- [6] M. M. Zayed and M. Shokair, "Modeling and simulation of optical wireless communication channels in IoUT considering water types turbulence and transmitter selection," *Scientific Reports*, vol. 15, no. 1, p. 28381, Aug. 2025, doi: 10.1038/s41598-025-10935-w.
- [7] N. Saeed, A. Celik, T. Y. Al-Naffouri, and M.-S. Alouini, "Underwater optical wireless communications, networking, and localization: A survey," *Ad Hoc Networks*, vol. 94, p. 101935, Jun. 2019, doi: 10.1016/j.adhoc.2019.101935.
- [8] Z. Zeng, S. Fu, H. Zhang, Y. Dong and J. Cheng, "A Survey of Underwater Optical Wireless Communications," in *IEEE Communications Surveys & Tutorials*, vol. 19, no. 1, pp. 204-238, Firstquarter 2017, doi: 10.1109/COMST.2016.2618841.
- [9] M. A. Khalighi and M. Uysal, "Survey on Free Space Optical Communication: A Communication Theory Perspective," in *IEEE Communications Surveys & Tutorials*, vol. 16, no. 4, pp. 2231-2258, Fourthquarter 2014, doi: 10.1109/COMST.2014.2329501.
- [10] I. Ramley, H. M. Alzayed, Y. Al-Hadeethi, M. Chen, and A. Z. Barasheed, "An Overview of Underwater Optical Wireless Communication Channel Simulations with a Focus on the Monte Carlo Method," *Mathematics*, vol. 12, no. 24, p. 3904, Dec. 2024, doi: 10.3390/math12243904.
- [11] D. Tsonev, S. Videv, and H. Haas, "Light fidelity (Li-Fi): towards all-optical networking," *Proceedings of SPIE, the International Society for Optical Engineering/Proceedings of SPIE*, vol. 9007, p. 900702, Dec. 2013, doi: 10.1117/12.2044649.
- [12] Jurong Bai et al., "Peak-to-average power ratio reduction for DCO-OFDM underwater optical wireless communication system based on an interleaving technique," *Optical Engineering*, vol. 57, no. 8, 086110, Aug 2018, doi: 10.1117/1.OE.57.8.086110.
- [13] A. Farhang, N. Marchetti and L. E. Doyle, "Low-Complexity Modem Design for GFDM," in *IEEE Transactions on Signal Processing*, vol. 64, no. 6, pp. 1507-1518, March15, 2016, doi: 10.1109/TSP.2015.2502546.
- [14] B. Farhang-Boroujeny, "OFDM Versus Filter Bank Multicarrier," in *IEEE Signal Processing Magazine*, vol. 28, no. 3, pp. 92-112, May 2011, doi: 10.1109/MSP.2011.940267.
- [15] A. A. R. Hema. and D. C. Diana., "Performance Evaluation of GFDM in Underwater Wireless Optical Communication," *2023 2nd International Conference on Vision Towards Emerging Trends in Communication and Networking Technologies (ViTECoN)*, Vellore, India, 2023, pp. 1-5, doi: 10.1109/ViTECoN58111.2023.10157613.
- [16] A. Fakchich et al., "MIMO techniques for robust underwater optical wireless communications by mitigating oceanic turbulence and transceiver misalignment," *papers.ssrn.com*, doi: 10.2139/ssrn.5786874.
- [17] M. Sliti and M. Garai, "Performance Analysis of MIMO-Underwater Optical Wireless Communication," *2023 28th Asia Pacific Conference on Communications (APCC)*, Sydney, Australia, 2023, pp. 301-306, doi: 10.1109/APCC60132.2023.10460667.

- [18] M. Wolny, E. Muller, and E. Tangdiongga, "Transmitters and receivers for high capacity indoor optical wireless communication," *Telecom*, vol. 6, no. 2, p. 26, Apr. 2025, doi: 10.3390/telecom6020026.
- [19] J. Li, J. Piao, B. Yang, J. Yan and Y. Wang, "A Real-Time Underwater Wireless Optical Communication System: Hardware Realization and LED Array Drive Circuit Design," *2019 Asia Communications and Photonics Conference (ACP)*, Chengdu, China, 2019, pp. 1-3.
- [20] R. Hema, S. Sudha, and K. Aarthi, "Performance studies of MIMO based DCO-OFDM in underwater wireless optical communication systems," *Journal of Marine Science and Technology*, vol. 26, no. 1, pp. 97–107, Apr. 2020, doi: 10.1007/s00773-020-00724-7.
- [21] M. Murad, I. A. Tasadduq, and P. Otero, "Coded-GFDM for reliable communication in underwater acoustic channels," *Sensors*, vol. 22, no. 7, p. 2639, Mar. 2022, doi: 10.3390/s22072639.
- [22] Z. Li, W. Li, K. Sun, D. Fan, and W. Cui, "Recent progress on underwater wireless communication methods and applications," *Journal of Marine Science and Engineering*, vol. 13, no. 8, p. 1505, Aug. 2025, doi: 10.3390/jmse13081505.
- [23] C. Pallavi and G. Sreenivasulu, "A Highly Compatible Optical/Acoustic Modem based on MIMO-OFDM for Underwater Wireless Communication using FPGA," *International Journal of Electrical and Electronics Research*, vol. 11, no. 4, pp. 993–1000, Nov. 2023, doi: 10.37391/ijeer.110417.
- [24] C. Pallavi and G. Sreenivasulu, "A hybrid optical-acoustic modem based on MIMO-OFDM for reliable data transmission in green underwater wireless communication," *Journal of VLSI Circuits and Systems*, vol. 6, no. 1, pp. 36–42, 2023, doi: 10.31838/jvcs/06.01.06.
- [25] C. H. Pallavi and G. Sreenivasulu, "A high speed underwater wireless communication through a novel hybrid Opto-Acoustic modem using MIMO-OFDM," *Instrumentation Mesure Métrologie*, vol. 20, no. 5, pp. 279–287, Oct. 2021, doi: 10.18280/i2m.200505.
- [26] Tejovathi Venati and Swarnalatha Sugali, "A Power-Efficient optical modem for reliable, Long-Distance communication using GFDM technology in underwater and terrestrial wireless systems," *International Journal of Computational and Experimental Science and Engineering*, vol. 11, no. 1, Feb. 2025, doi: 10.22399/ijcesen.1034.